The Plant Cell, Vol. 25: 2417–2428, July 2013, www.plantcell.org 

LARGE-SCALE BIOLOGY ARTICLE

# Plant MicroRNAs Display Differential 3′ Truncation and Tailing Modifications That Are ARGONAUTE1 Dependent and Conserved Across Species[W]

**Jixian Zhai,[a] Yuanyuan Zhao,[b] Stacey A. Simon,[a] Sheng Huang,[c] Katherine Petsch,[d] Siwaret Arikit,[a] Manoj Pillay,[a,1] Lijuan Ji,[b] Meng Xie,[e] Xiaofeng Cao,[f] Bin Yu,[e] Marja Timmermans,[d] Bing Yang,[c] Xuemei Chen,[b,g] and Blake C. Meyers[a,2]**

[a] Department of Plant and Soil Sciences, Delaware Biotechnology Institute, University of Delaware, Newark, Delaware 19711
[b] Department of Botany and Plant Sciences, Institute of Integrative Genome Biology, University of California, Riverside, California 92521
[c] Department of Genetics, Development, and Cell Biology, Iowa State University, Ames, Iowa 50011
[d] Cold Spring Harbor Laboratory, Cold Spring Harbor, New York 11724
[e] Center for Plant Science Innovation and School of Biological Sciences, University of Nebraska, Lincoln, Nebraska 68588
[f] State Key Laboratory of Plant Genomics and National Center for Plant Gene Research, Institute of Genetics and Developmental Biology, Chinese Academy of Sciences, Beijing 100101, China
[g] Howard Hughes Medical Institute, University of California, Riverside, California 92521

ORCID ID: 0000-0003-3436-6097 (B.C.M.).

**Plant small RNAs are 3′ methylated by the methyltransferase HUA1 ENHANCER1 (HEN1). In plant *hen1* mutants, 3′ modifications of small RNAs, including oligo-uridylation (tailing), are associated with accelerated degradation of microRNAs (miRNAs). By sequencing small RNAs of the wild type and *hen1* mutants from *Arabidopsis thaliana*, rice (*Oryza sativa*), and maize (*Zea mays*), we found 3′ truncation prior to tailing is widespread in these mutants. Moreover, the patterns of miRNA truncation and tailing differ substantially among miRNA families but are conserved across species. The same patterns are also observable in wild-type libraries from a broad range of species, only at lower abundances. ARGONAUTE (AGO1), even with defective slicer activity, can bind these truncated and tailed variants of miRNAs. An *ago1* mutation in *hen1* suppressed such 3′ modifications, indicating that they occur while miRNAs are in association with AGO1, either during or after RNA-induced silencing complex assembly. Our results showed AGO1-bound miRNAs are actively 3′ truncated and tailed, possibly reflecting the activity of cofactors acting in conserved patterns in miRNA degradation.**

## INTRODUCTION

The stability and function of small RNAs (sRNAs) are affected by various modifications, such as methylation, uridylation, adenylation, and RNA editing (Kim et al., 2010; Ji and Chen, 2012). Plant microRNAs (miRNAs) pair with their targets near-perfectly and are 3′ protected by methylation (Voinnet, 2009); by contrast, animal miRNAs are unmethylated and typically partially complementary to their mRNA targets via the short seed region at the 5′ end (Bartel, 2009) and can be truncated and tailed when extensively matched by a target RNA (Ameres et al., 2010).

*HUA1 ENHANCER1* (*HEN1*), first identified in a screen for floral mutants in *Arabidopsis thaliana*, was later characterized as a methyltransferase that adds a 2′-*O*-methyl group to the 3′ terminal nucleotide of miRNAs and small interfering RNAs (siRNAs) (Li et al., 2005; Yu et al., 2005). Structural analysis determined that HEN1 specifically recognizes the sRNA duplex as a substrate (Huang et al., 2009). In *hen1* mutant backgrounds, miRNAs examined by RNA gel blot analysis exhibit unusual length heterogeneity and the abundance of most miRNAs is considerably reduced (Li et al., 2005; Yu et al., 2005). Comparisons performed by cloning and sequencing individual miRNAs in wild-type and *hen1-1* backgrounds showed the addition of predominantly uridine (U) nucleotides at the 3′ end of some miRNAs in a *hen1-1* mutant (Li et al., 2005). The U-rich tail of unmethylated miRNAs in *Arabidopsis hen1* mutants is added by nucleotidyl transferase HEN1 SUPPRESSOR1 (HESO1), whose mutation can partially rescue the phenotype of *hen1* mutants by increasing miRNA accumulation (Ren et al., 2012; Zhao et al., 2012b). A family of SMALL RNA DEGRADING NUCLEASE (SDN) proteins was identified in *Arabidopsis* that degrades mature miRNAs (Ramachandran and Chen, 2008). Work on plant HEN1 has been primarily performed in *Arabidopsis*, the characterization of *wavy leaf1* (*waf1*) mutants in rice (*Oryza sativa*), the ortholog of *Arabidopsis*

[1] Current address: Lawrence Berkeley National Laboratory, Berkeley, CA 94720.
[2] Address correspondence to meyers@dbi.udel.edu.
The author responsible for distribution of materials integral to the findings presented in this article in accordance with the policy described in the Instructions for Authors (www.plantcell.org) is: Blake C. Meyers (meyers@dbi.udel.edu).
[W] Online version contains Web-only data.
www.plantcell.org/cgi/doi/10.1105/tpc.113.114603

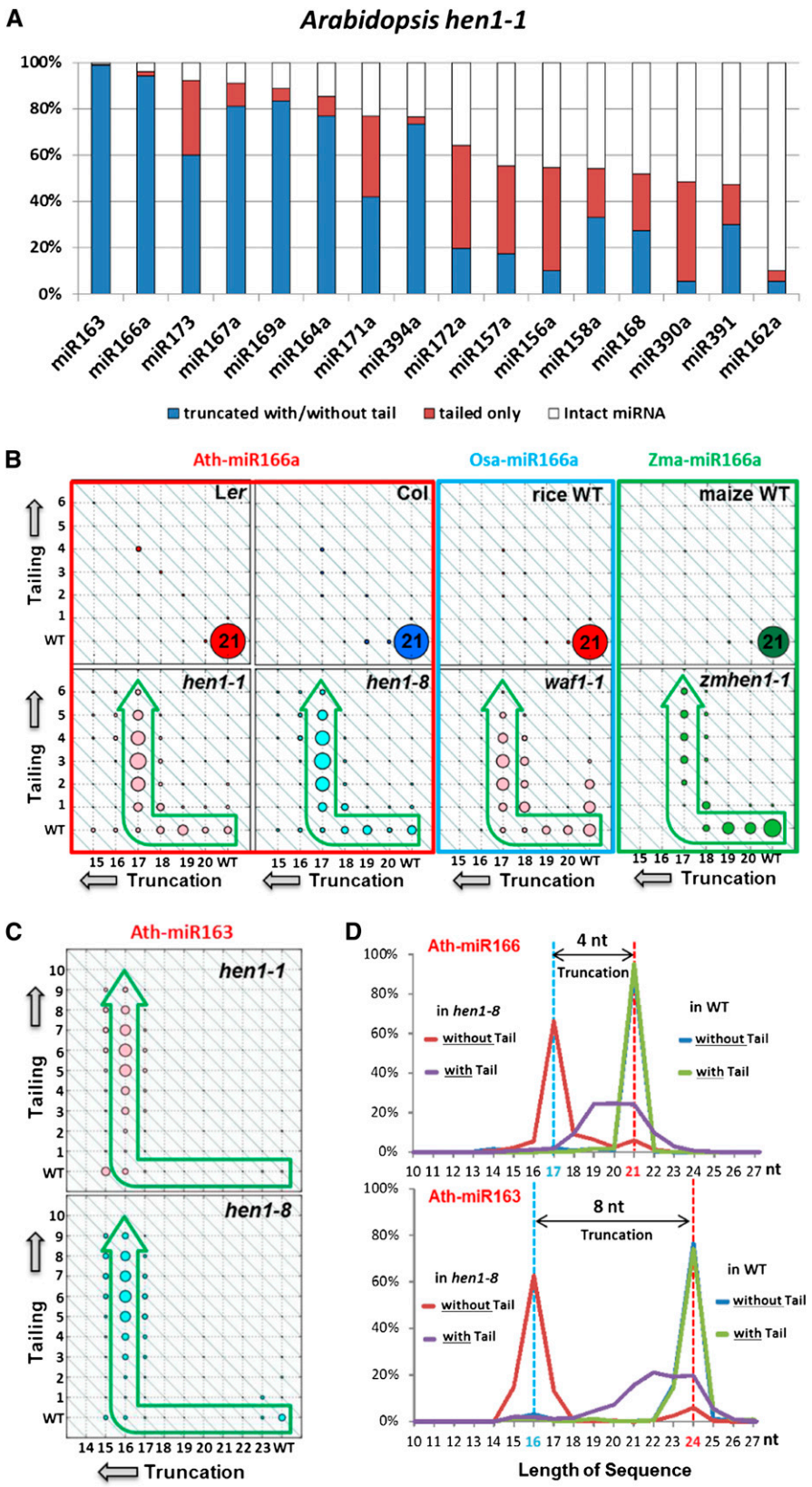


**Figure 1.** miRNAs Are Differentially Truncated and Tailed in *hen1* Mutants.

HEN1 (Abe et al., 2010), and a newly identified *hen1* mutant in maize (*Zea mays*) represent an opportunity to expand our understanding of HEN1 function into monocots. In this study, we used deep sequencing to characterize the extent of 3′ modification of sRNAs in both the wild type and *hen1* mutants of *Arabidopsis*, rice, and maize and found that, in contrast with the previous understanding that all miRNAs are simply shortened or tailed in *hen1*, the pattern of 3′ modifications varied substantially among miRNA families, and both truncation and tailing are AGO1 dependent.

## RESULTS

### Sequencing of sRNAs from Plant *hen1* Mutants

To date, miRNAs in *hen1* mutants were mainly investigated via RNA gel blot hybridization, which is low throughput and cannot reveal the changes to miRNA sequence composition. Cloning followed by Sanger sequencing of miR173 and miR167 in At-*hen1-1* revealed truncation and one to five nucleotides of uridylation at the 3′ end of miRNAs (Li et al., 2005). With the tremendous advances in high-throughput sequencing technologies, it is possible systematically to study sRNA population in *hen1* mutants with unprecedented depth. Several *hen1* mutant alleles have been identified in both *Arabidopsis* and rice (Chen et al., 2002; Abe et al., 2010; Yu et al., 2010). In this analysis, we analyzed three *hen1* mutant alleles in *Arabidopsis*, three *hen1* alleles in rice, and a newly identified *hen1* mutant in maize. This includes a new mutant allele of the rice *HEN1* gene (Os-*hen1-3*) from the Korean (POSTEC) rice T-DNA mutant population (Jeong et al., 2002). This mutant, with a T-DNA insertion that disrupts the Os-*HEN1* open reading frame 97 bp upstream of the stop codon, has a similar phenotype to the *wavy leaf* mutants (see Supplemental Figure 1 online). We also identified the *hen1* mutant allele in maize (Zm-*hen1-1*) from the UniformMu population with an insertion in the first exon. In the native W22 background, these plants displayed a shoot-meristemless phenotype like many rice *waf1* plants, and we therefore analyzed seedlings from a backcross to B73, which displayed a weaker phenotype (see Supplemental Figure 2 online). We sequenced by Illumina technology sRNAs from all of these plant materials (see Supplemental Table 1 online).

In addition to reduced sRNA levels in *hen1* mutants (Li et al., 2005; Yu et al., 2005), we observed that the size distribution of sRNAs in *hen1* differed from the wild type in all three species, with reduced 21- and 24-nucleotide peaks, accompanied by an increase in the relative proportion of other sRNA sizes (see Supplemental Figure 3 online). This size shift could be due to sRNA truncation, polyuridylation, or a combination of both. To analyze the sRNA derivatives, we devised an informatics pipeline as follows (Zhai and Meyers, 2013): First, each non-genome-matched sRNA read was divided into two parts, viz. the longest 5′ genome-matched component head portion and a 3′ tail portion (for the reads that perfectly mapped to the genome we assumed there was no tail); next, focusing first on miRNAs, we aligned the head portion of the reads to each miRBase-annotated miRNA (allowing only perfect matches) to determine the extent of tailing (addition of nontemplated 3′ nucleotides) and truncation (shortening of the miRNA from the 3′ end, usually prior to tailing). This calculated the degree and characteristics of both truncation and tailing for annotated *Arabidopsis*, rice, and maize miRNAs.

### miRNAs Are Differentially Truncated and Uridylated in *hen1* Mutants

Consistent with the previous reports of miRNAs in *hen1* mutants (Li et al., 2005; Yu et al., 2005; Yu et al., 2010), we were able to

**Figure 1.** (continued).

In both **(B)** and **(C)**, the "truncation and tailing matrix", the *x* axis represents the length of the 5′ genome-matched component (head) of a particular miRNA related sequence; the *y* axis represents the length of the tail added to the head, mostly through uridylation. The miRBase-annotated miRNA sequence is considered to have no truncation or tail (e.g., like the wild type [WT]) and therefore is positioned at (WT, WT) in the matrix, while a miR166a-related sequence identified with a 17-nucleotide head (four-nucleotide truncation) and three-nucleotide tail will be positioned at (17, 3) in **(A)**. The area within the circle for each position indicates the relative abundance of all sRNAs matching to that particular position. Different colors are used to indicate different genotypes. Positions on the same diagonal line have the same actual length; in case of miR166a, position (WT, WT) and position (17, 4) are on the same line, and both are 21 nucleotides in actual length.

**(A)** Summary of truncation and tailing patterns of selected, abundant *Arabidopsis* miRNAs in *hen1-1*. Blue, percentage of truncated miRNA variants (with or without tailing); red, percentage of variants that are only tailed; white, the miRBase-annotated miRNA sequence is considered intact. miR163 and miR166 were the most truncated and tailed, while miR162 showed minimal truncation and uridylation in *hen1-1*.

**(B)** miR166a is mostly truncated to 17 nucleotides prior to being tailed to larger sizes, with an almost identical pattern from both *hen1-1* and *hen1-8*. Shown on the left are truncation and tailing patterns of miR166a (21 nucleotides) in L*er*, *hen1-1*, Columbia, and *hen1-8*. The green, bent arrow suggests a way to read the plot. On the right, the truncation and tailing pattern specific to miR166 and observed in *Arabidopsis* is also conserved in rice *waf1-1* and maize *hen1-1*.

**(C)** miR163 is truncated to ~16 nucleotides from 24 nucleotides and is tailed back to ~24 nucleotides. Shown are truncation and tailing patterns in *hen1-1* and *hen1-8* for miR163 (24 nucleotides). The patterns for these miRNAs in Columbia and L*er* (not shown) were predominately at the (WT, WT) position.

**(D)** Size distributions of head (without tail) and full-length sRNA in Columbia and *hen1-8* for miR166a (above) and miR163 (below). The *x* axis represents the length of either the head or sRNA; the *y* axis represents the proportion of head or sRNA at each size. In Columbia, head and sRNA are almost completely overlapping because the very low levels of truncation and tailing. miR166a is primarily truncated from 21 nucleotides (nt) to 17 nucleotides (blue on *x* axis), then tailed strongly until its original size of 21 nucleotides (red on *x* axis); miR163 is primarily truncated from 24 nucleotides down to ~16 nucleotides (blue on *x* axis) with an eight-nucleotide truncation, then tailed to a size of 24 nucleotides (red on *x* axis).

identify a high level of tailing for many miRNAs, predominantly via uridylation. However, contrary to the previous impression that miRNAs in *hen1* mutants are simply tailed or slightly shortened, we found that the degree of 3′ modifications varied substantially among different miRNA families (Figure 1A). Additionally, we observed heavy truncation prior to uridylation for many miRNAs (see Supplemental Data Set 1 online). Because in many cases this restored a length similar to the wild-type miRNA (see below), the combination of heavy truncation and uridylation cannot be revealed by hybridization-based methods like RNA gel blots. The

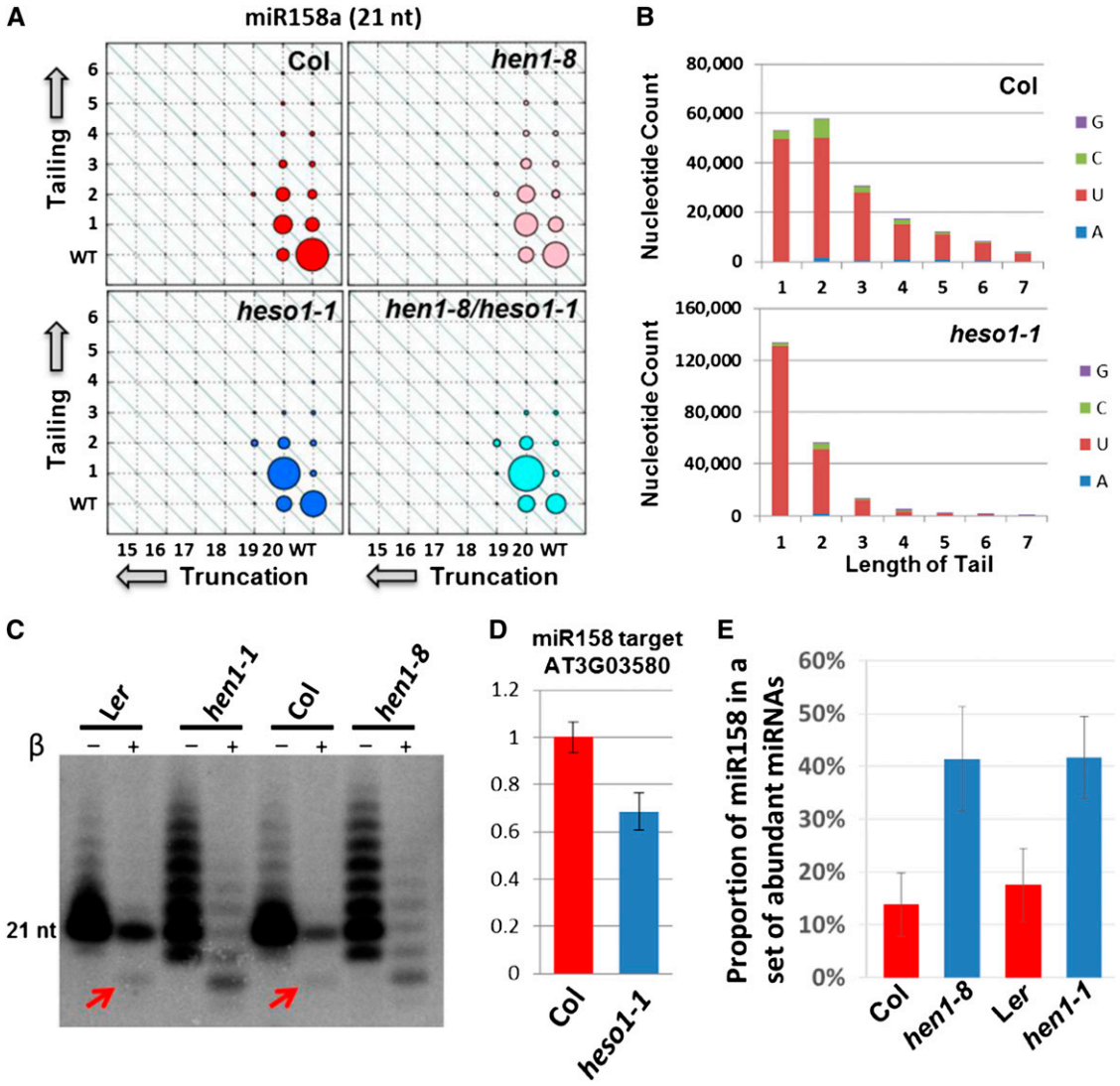


**Figure 2.** *Arabidopsis* miR158 Is Partially Unmethylated in the Wild Type and Subject to Truncation and Uridylation.

**(A)** Levels of miR158 truncation and tailing are similar in *hen1-8* and the wild type (WT) and are reduced by the *heso1-1* mutation in the background of either a functional *HEN1* allele or in a *hen1-1* background. See Figure 1 for the interpretation of matrix. nt, nucleotides.

**(B)** The length of miR158 tail is shifted to smaller sizes in the *heso1-1* mutant compared with Columbia (Col), but the composition is unchanged. The tails of the miR158-derived reads were grouped by their length (position on *x* axis); the count for the composition of each type of ribonucleotide was as indicated (*y* axis).

**(C)** miR158 is partially unmethylated in both Columbia and L*er* wild types and thus subject to truncation and tailing. "β" indicates β-elimination treatment, after which unmethylated sRNAs run approximately two nucleotides faster than methylated sRNAs. Red arrows indicate the unmethylated miR158 after β-elimination in both Columbia and L*er*.

**(D)** The expression level of miR158 target, AT3G03580, is decreased in a *heso1-1* single mutant relative to the wild-type Columbia-0 level, as measured by quantitative RT-PCR, and error bars represent the estimated SD from three replicated experiments.

**(E)** The proportion of the most abundant miRNAs comprised by miR158 derivatives in replicated wild-type and *hen1 Arabidopsis* sRNA libraries; miR158 derivatives are relatively enriched in *hen1* mutants compared with the wild type. The *y* axis shows the mean values for the proportion of miR158 derivatives from three replicated libraries for each genotype, and error bars represent the estimated SD.

unique patterns described below for different miRNA families were highly reproducible in both *hen1-1* and *hen1-8*, mutant alleles isolated in two different *Arabidopsis* accessions (Figures 1B and 1C; see Supplemental Data Set 1 online) and are even conserved across plant species (Figure 1B; see Supplemental Figure 4 and Supplemental Data Set 2 online), suggesting that structural, sequence-dependent, or other as yet unknown effects specify the 3′ modifications resulting from reduced HEN1 levels.

miR165/6 (21 nucleotides) family members play important roles in plant development by targeting type III HD-Zip genes *REVOLUTA*, *PHABULOSA*, and *PHAVOLUTA* to regulate leaf polarity and stem cell identity (Mallory et al., 2004; Williams et al., 2005). In *hen1* mutants, we observed that miR166 is first truncated to ~17 nucleotides without any tailing and then is uridylated to ~21 nucleotides, its original length (Figure 1B). Our pipeline defined the truncation to ~17 nucleotides, but it is possible that the truncation was to ~15 nucleotides (16th and 17th nucleotides of miR166a are both uridine). Since plant miRNAs are generally 21 nucleotides, we wondered if the tailing back to 21 nucleotides is a universal feature. To test this, we analyzed miR163, which is unique because of its unusual 24-nucleotide length, due to two asymmetric bulges on the miRNA strand of the duplex (Kurihara and Watanabe, 2004). In *Arabidopsis hen1* mutants, miR163 has the longest truncation among all miRNAs; it is truncated by eight nucleotides to a predominant length of 16 nucleotides before uridylation, and then it is tailed back to its original length at ~24 nucleotides (Figures 1C and 1D). This ability to regain the original miRNA size after truncation and tailing implies a memory of the original length. These two examples also suggest that the truncation activity, possibly performed by the SDN family of exonucleases (Ramachandran and Chen, 2008), in cases like miR166 and miR163 could be upstream of the uridylation activity, as tailing may not occur until the miRNA is shortened to a certain length. Other patterns were also apparent, for example, miR156, which targets SPL genes to regulate developmental time (Poethig, 2009), and miR172, which represses the translation of AP2-domain transcription factors

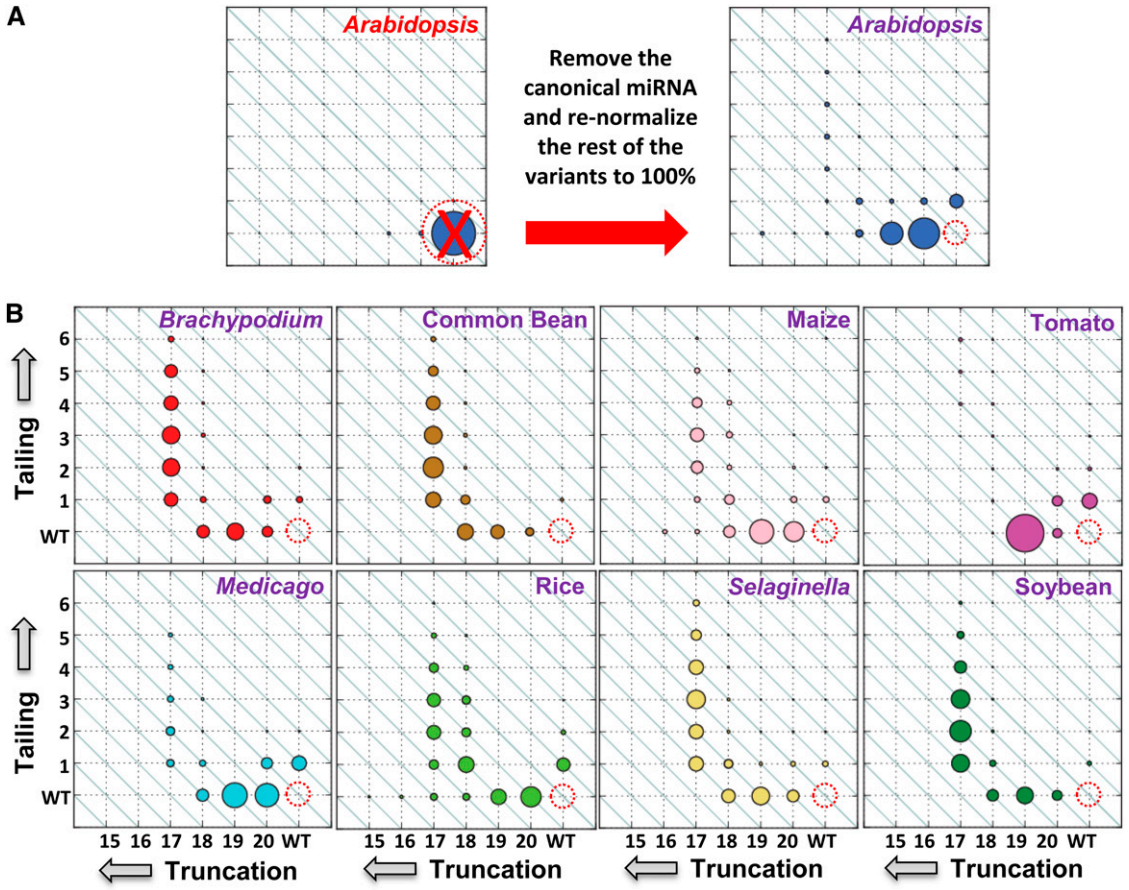


**Figure 3.** miR166 Is Naturally Truncated and Tailed in a Broad Range of Wild-Type Plant Species.

**(A)** To generate the data in **(B)**, the canonical miRNA was removed and all remaining variants were renormalized to add to 100%, enriching the signal for 3′ modified variants. The hollowed red circle indicates that the canonical miRNA abundance was removed. The data in this panel are from the same experiment as Figure 2.

**(B)** Truncated and polyuridylated 3′ variants of miR166a were examined in eight different plant species (libraries listed in Supplemental Table 2 online). WT, the wild type.

(Chen, 2009), were tailed but with little truncation; the *Dicer-like1* -targeting miR162 (Xie et al., 2003) was only slightly tailed or truncated (somewhat protected) (see Supplemental Figure 4 online). Thus, these patterns are highly conserved among different *hen1* alleles from different plant species.

### 3′ Modified miRNAs in Wild-Type Plants

Prior analyses suggested that plant miRNAs are fully methylated in vivo by HEN1, which protects them from 3′ uridylation (Li et al., 2005; Yu et al., 2005). While our sequencing results showed that miRNAs are predominately protected in the wild type from truncation and tailing, we found some exceptions. Even in an *Arabidopsis* wild-type background with functional *HEN1*, miR158 was both truncated and tailed at substantial levels, levels somewhat similar to this miRNA in the *hen1* mutants (Figure 2A). HEN1 SUPPRESSOR1 (HESO1) is a nucleotidyltransferase that can uridylate unmethylated miRNAs and promote their degradation (Ren et al., 2012; Zhao et al., 2012b). *Arabidopsis HESO1* was identified because its loss of function can suppress the phenotype of *hen1-8* by reducing levels of uridylation and increasing miRNA accumulation in general. HESO1 can only add nucleotides (predominantly uridine) to the 3′ terminus of unmethylated RNA, as 2′-*O*-methylation blocks its activity (Zhao et al., 2012b). In the *heso1-1* mutant, we found that the level of tailing of miR158 is dramatically reduced (Figure 2A), and the length of the miR158 tail was shifted to smaller sizes because of reduced uridylation (Figure 2B). However, miR158 is not unique, as miR319a is also tailed in wild-type *Arabidopsis* and its modification is suppressed in *heso1-1* (Zhao et al., 2012b).

The fact that miR158 is uridylated in the wild type and its tailing pattern is impacted by *heso1-1* suggests that miR158 might be partially unmethylated in the wild type. To assess miR158 methylation in the wild type, we performed a β-elimination experiment, which increases the mobility of only unmethylated sRNAs by approximately two nucleotides in RNA gel blots (Alefelder et al., 1998; Hutvágner et al., 2001). Consistent with our hypothesis, a portion of miR158 in the wild type ran two nucleotides faster, the same as the unmethylated miR158 in *hen1* mutants (Figure 2C). We concluded that in the wild type *Arabidopsis* miR158 is characterized by incomplete 2′-*O*-methylation and consequently is truncated and uridylated. Since uridylation leads to degradation of miRNAs, we asked whether miR158 activity is modulated by its incomplete methylation and uridylation. Indeed, the expression level of the miR158 target, AT3G03580, is decreased in the *heso1-1* mutant (Figure 2D), suggesting that miR158 function is partially suppressed in the wild type via destabilization. To assess the possibility of destabilization, we examined the proportion of the most abundant miRNAs comprised by miR158 derivatives in replicated wild-type and *hen1 Arabidopsis* sRNA libraries (see Supplemental Table 1 online). This showed that miR158 levels comprise ~14 to 17% of the total in the wild type (Columbia-0 and Landsberg erecta [L*er*]) but 41% in both *hen1-1* and *hen1-8* (Figure 2E). This enrichment suggests that in a *hen1* background in which all other miRNAs are destabilized, miR158 is relatively less impacted by the loss of HEN1.

The level of 3′ modifications observed in miR158 and miR319 led us to look more carefully at published sequencing data in wild-type plants for many other species, including monocots (maize, *Brachypodium*, and rice), other eudicots (soybean [*Glycine max*], *Medicago*, and tomato [*Solanum lycopersicum*]), and even the basal land plant *Selaginella*. We picked the three most representative sequence variants of the truncated and tailed forms of miR166 in the *Arabidopsis hen1* mutant to search in wild-type sRNA libraries, and we found them present in all the species examined (see Supplemental Table 2 online). Next, we

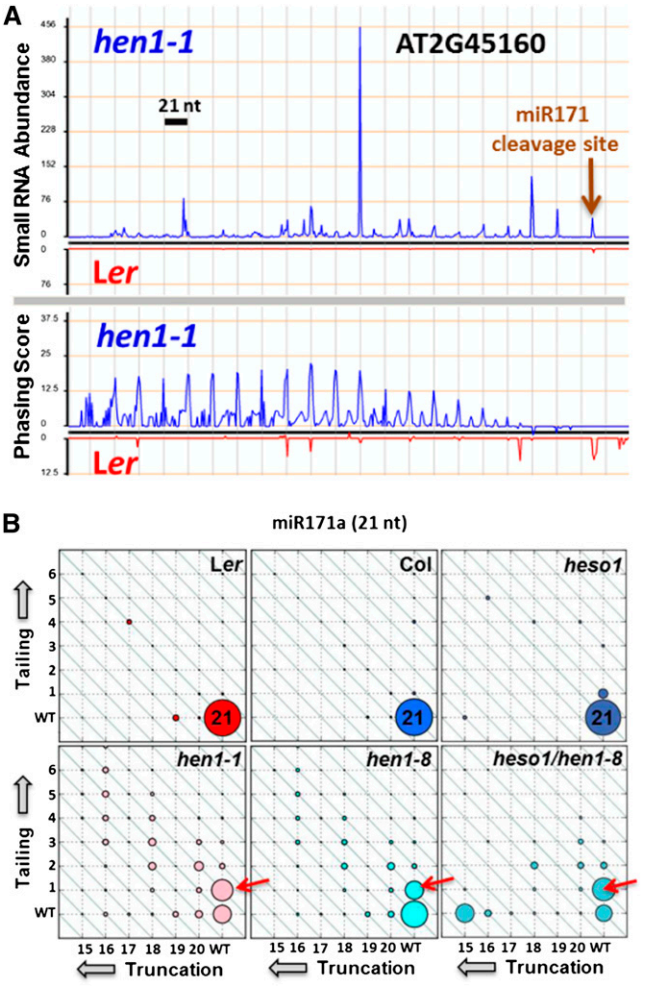


**Figure 4.** *Arabidopsis* miR171a Is Tailed to 22 Nucleotides and Triggers Phased, Secondary siRNAs at Its Target in *hen1* Mutants.

**(A)** A 22-nucleotide (nt) uridylated miR171a variant triggers production of phased, secondary siRNAs in *hen1-1*. Top panel, sRNA abundances; bottom panel, phasing score distributions for the target At2g45160 in *hen1-1* (blue) and L*er* (red); abundances are normalized to TP2M, with the brown arrowhead pointing to the miRNA cleavage site, which is perfectly in phase (21-nucleotide intervals) with the sRNA distribution.
**(B)** miR171a is mostly uridylated by one nucleotide to 22 nucleotides in both *hen1-1* and *hen1-8*. Truncation and tailing patterns of miR171a (21 nucleotides) in various genotypes, as described in Figure 1. Col, Columbia; WT, the wild type.

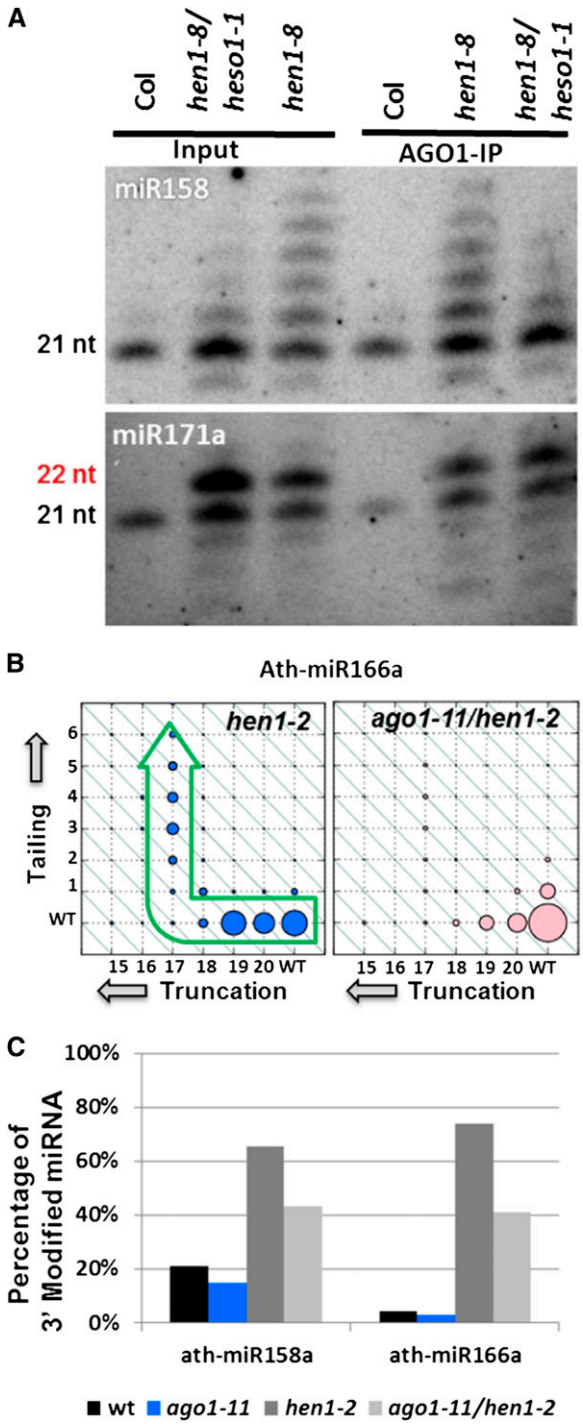


**Figure 5.** AGO1 Binding and Involvement in 3′ Truncation and Tailing of *Arabidopsis* miRNAs.

**(A)** AGO1 binding of miRNA variants shown by RNA gel blots using input and AGO1 IP-derived sRNAs from Columbia (Col), *hen1-8*, and *hen1-8 heso1-1*. Top panel: The truncated and uridylated miR158 variants. Bottom panel: The canonical 21-nucleotide (nt) miR171a and its primarily 22-nucleotide variant.

**(B)** Measurement of truncated and tailed miR166a variants in *Arabidopsis* in either *hen1-2* (left) or a double mutant of *ago1-11* and *hen1-2* (right). In the double mutant, truncation and tailing is suppressed.

**(C)** Proportion of 3′ modified variants of two *Arabidopsis* miRNAs in single and double mutants of *ago1-11* and *hen1-2* (as labeled).

examined 3′ truncation and tailing patterns of miR166 variants from these wild-type species, removing from consideration the canonical miR166 to emphasize the truncated and tailed variants (Figure 3A). Across the broad range of species examined, the patterns of truncation and tailing are strikingly similar, with slightly reduced truncation and tailing observed only in tomato (Figure 3B). This suggests that the truncation and tailing of miR166 is ancient and highly conserved across plant species and only becomes more visible in a *hen1* mutant background. Thus, wild-type plants show truncation and tailing of miRNAs enhanced in *hen1* (e.g., miR166), and some miRNAs are naturally 3′ modified at moderate levels (e.g., miR158 and miR319).

### miR171a Is Uridylated from 21 to 22 Nucleotides in *hen1*, Triggering Phased, Secondary siRNA Production

Many miRNAs are truncated and uridylated to exhibit heterogeneous sizes in *hen1* mutants, which includes 22 nucleotides, a length perhaps sufficient to trigger at their targets the production of secondary siRNAs (Chen et al., 2010; Cuperus et al., 2010). These secondary siRNAs are distributed in fixed intervals (a phase of usually 21 nucleotides) due to consistent and precise miRNA cleavage. Given that most *Arabidopsis* miRNAs are 21 nucleotides in the wild-type background, it is possible that some or many miRNA targets produce tasiRNAs in the *hen1* mutant because the miRNA variants that are tailed to 22 nucleotides. We performed a genome-wide analysis of sRNA phasing (Zhai et al., 2011) with the *hen1* mutant sRNA libraries. Only the two loci AT2G45160 and AT3G60630, both of which regulate the development of shoot meristem (Schulze et al., 2010), produced phased siRNAs in *hen1* mutants but not the wild type (Figure 4A; see Supplemental Figure 5 online). These genes are both the predicted targets of miR170/171a (see Supplemental Figure 5 online). Both miR170 and miR171a were primarily tailed to and stabilized at 22 nucleotides in *hen1* (Figure 4B; see Supplemental Data Set 1 online). However, 22-nucleotide variants of other miRNAs that are 21 or 20 nucleotides in the wild type did not gain the ability to trigger phased siRNAs at their targets (data not shown). Thus, in *hen1*, an sRNA length of 22 nucleotides is necessary but not sufficient to trigger phased siRNA production. Manavella et al. (2012) previously described that both (1) RNA-induced Silencing Complex (RISC) reprogramming by asymmetric structure of miRNA/miRNA* duplex can enable them to trigger secondary siRNAs, and (2) miR170/171 lack such asymmetry on their duplex but were found in ARGONAUTE7 immunoprecipitation (AGO7-IP) sRNAs, which might permit it to initiate secondary siRNA production, like the AGO7-bound miR390. Curiously, in the double mutant *heso1-1 hen1-8*, the 22-nucleotide variant of miR171a was unaffected (Figure 4B); thus, the single 3′ nucleotide addition must be added by a different enzyme. We checked the miR171c/d family

members, which are 3′ shifted by three nucleotides relative to miR170/171a and show different patterns of 3′ modifications (e.g., not consistently 22 nucleotides; see Supplemental Data Set 1 online).

### Mutations in *AGO1* Suppress the Truncation and Tailing of miRNAs

Since most plant miRNAs are bound by AGO1, we next wondered about the role of AGO1 in 3′ modifications of miRNAs, asking the following: (1) Are 3′ modified miRNAs competent to be bound by AGO1? (2) If they are bound, does AGO1 influence 3′ modifications? In *Drosophila melanogaster*, extensive matching between Argonaute1-bound miRNA and its target destabilize miRNA through 3′ truncation and tailing (Ameres et al., 2010). By RNA gel blots, immunoprecipitation (IP) of AGO1 showed that it bound the variants of all sizes for miR158 and miR171a in an *Arabidopsis hen1* background, with the binding of these variants unaffected in the *heso1-1 hen1-8* double mutant (Figure 5A). Similar observations were made for miR165/6 and miR167 (Zhao et al., 2012a). Sequenced sRNAs from AGO1 IP further confirm the binding of 3′ modified sRNAs in *hen1* and *hen1 heso1* for many other miRNAs (see Supplemental Figure 6A online). To answer whether AGO1-bound miRNAs were actively modified while in association with AGO1 or these miRNAs were already modified prior to AGO1 loading, we sequenced sRNAs from *ago1-11* (a weak allele), *hen1-2*, and an *ago1-11 hen1-2* double mutant (see Supplemental Table 1 online). Truncation and tailing of many miRNAs in *hen1* was suppressed by *ago1* mutants, for different alleles of both genes (Figures 5B and 5C; see Supplemental Figure 6C online), suggesting that 3′ modifications of unmethylated miRNAs occur after AGO1 loading. Consistent with this, AGO1 and HESO1 colocalize (G. Ren, M. Xie, C. Vinovskis, and B. Yu, unpublished data). We also examined immunoprecipitated miRNAs from an AGO1 slicer-defective mutant (Carbonell et al., 2012) and observed little impact on miR158 tailing, indicating that AGO1 slicer activity is not required to modulate 3′ modifications (see Supplemental Figure 6B online). Such 3′ modifications occurring without target cleavage are reminiscent of *D. melanogaster* miRNA truncation and tailing that occurs when extensively matched by a synthetic target mRNA (Ameres et al., 2010). In contrast with the *heso1 hen1* double mutant, which is impacted only in 3′ tailing (Zhao et al., 2012b), in *ago1-11 hen1-2*, both truncation and tailing are reduced (Figure 5B), suggesting that AGO1 not only interacts with HESO1 but may have a role in modulating 3′ exonucleolytic activity.

### Sequence Determinants of miRNA 3′ Modifications

A key question for our study is the nature of the determinants impacting the 3′ modifications. The sRNA sequence presumably has a role, which could reflect individual nucleotides or structural characteristics of the miRNA duplex. We sought to investigate such impacts using miRNA family members with similar but distinguishable sequence. The 5′-most nucleotide of a miRNA is a primary determinant for the AGO onto which the miRNA will be loaded (Mi et al., 2008). The related miR158a and miR158b differ only by the 5′ nucleotide, yet have identical 3′ modifications (Figure 6A). Meanwhile, miR170/171a are closely related to miR171b/c, with a conserved core sequence, but a processing shift of three nucleotides alters the 3′ modifications (Figure 6B). Together, these data suggest that the 5′ and middle part of the miRNA are not essential for shaping the 3′ truncation and tailing pattern, leaving the 3′-end sequence as a more promising candidate. Indeed, miR166 and miR169, which share similar sequences at the 3′ end but different in their 5′ and

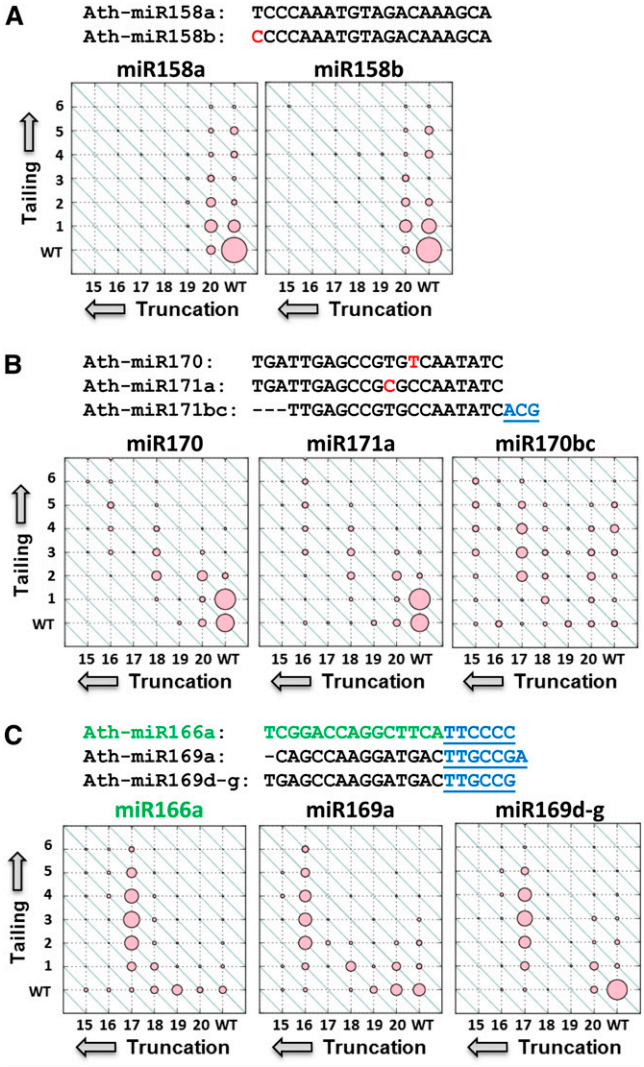


**Figure 6.** Impacts of Sequence on miRNA Truncation and Tailing (in *Arabidopsis hen1-1*).

Three sets of miRNAs were selected to test whether the 5′ end, middle region, or 3′ end of the miRNA influences 3′ truncation and tailing. In each case, an alignment above highlights the difference of the selected miRNAs, and the panels below show the pattern of 3′ truncation and tailing in the *Arabidopsis hen1-1* mutant. The sets of miRNAs and the three regions of the miRNA are as follows: miR158 family (5′ end) **(A)**, miR171 family (middle part and 3′ end) **(B)**, and miR166 and miR169 (3′ end) **(C)**. WT, the wild type.

middle regions, are almost identical in their truncation and tailing pattern (Figure 6C), indicating that the 3′ end sequence may substantially influence the patterns of miRNA 3′ modification.

### siRNAs Are Truncated and Uridylated in *hen1* Mutants

Previous studies on individual sRNAs have shown that 24-nucleotide heterochromatic siRNAs (hc-siRNAs) are uridylated and decreased in abundance in *hen1* mutants (Li et al., 2005), and their uridylation is also impacted by a *heso1* mutation, confirmed in the *heso1-1 hen1-8* background (Zhao et al., 2012b). To systematically study the impact of the *hen1* mutation on hc-siRNAs, we mapped the genome-matched components of sRNAs (the head portion) to annotated transposable elements to enrich for 24-nucleotide hc-siRNAs and filter out miRNAs and other types of sRNAs (such as trans-acting siRNAs). As expected, in the wild type, almost all the sRNAs that mapped to the transposable elements were predominately 24 nucleotides in length; in both *hen1-1* and *hen1-8* mutants, the proportion of 23- and 25-nucleotide variants increased relative to 24-nucleotide siRNAs, probably reflecting both truncation and tailing of these hc-siRNAs (see Supplemental Figure 7 online). Although the abundance of hc-siRNAs is drastically altered in the mutant background (Yu et al., 2010), the overall size distribution of hc-siRNAs in *hen1* was only moderately more dispersed from the 24-nucleotide peak (see Supplemental Figure 7 online), suggesting a more stringent size constraint on the 24-nucleotide hc-siRNAs than the AGO1-bound miRNAs. This constraint could result from properties of AGO4, the AGO protein that binds most hc-siRNAs and acts in transcriptional silencing (Zilberman et al., 2004; Qi et al., 2006). We also examined tasiRNAs from *Arabidopsis* and observed that two abundant *TAS3* sRNAs are highly truncated and tailed in *hen1* mutants, but with different patterns (see Supplemental Data Set 1 online). Thus, *hen1* mutations broadly affect sRNAs via increased 3′ modifications.

## DISCUSSION

### The Process of Plant miRNA 3′ Truncation and Tailing

When and where do these 3′ sRNA modifications occur? Our data showing that *ago1* mutations suppress both truncation and tailing indicate that the 3′ modifications take place in association with AGO1, either during the process of AGO1 loading or in the assembled RISC. Other data support this, including a recent demonstration of direct AGO1–HESO1 interaction (G. Ren, M. Xie, C. Vinovskis, and B. Yu, unpublished data) and a demonstration that near-perfect miRNA-mRNA target pairing can trigger 3′ modifications of *D. melanogaster* miRNAs (Ameres et al., 2010).

To achieve differential truncation and tailing, the machinery responsible for sRNA modifications must be able to distinguish different miRNAs after their loading into AGO1. The distinct truncation and tailing patterns of miR166 and miR163, and especially the fact that they are uridylated back to their original length (21 and 24 nucleotides, respectively) (Figure 1D), show that the truncation and tailing pattern is specified by the miRNA sequence. Our analysis of similar miRNAs and their 3′ modifications suggest that it is the 3′ sequence that influences the patterns of miRNA 3′ modification. Structural analyses of a binary complex of a bacterial Argonaute bound to a 5′-phosphorylated

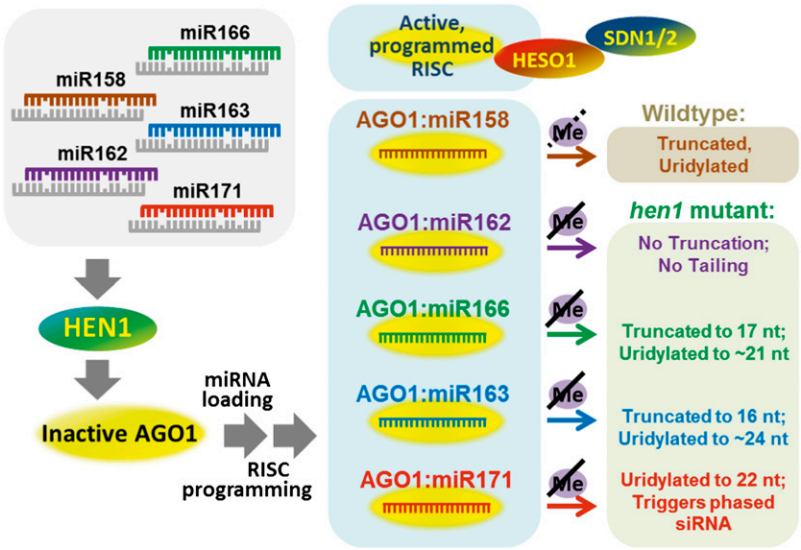


**Figure 7.** Model for the Diverse Patterns of Truncation and Uridylation of miRNAs in *hen1* Mutants.

Model for differentiated truncation and tailing patterns of miRNAs. AGO1 (or RISC) remains inactive/undifferentiated until the loading of the miRNA duplex. During loading, RISC is programmed to accommodate the particular miRNA to which it binds and thus lead to specialized miRNA-containing RISCs that exhibit various degrees of truncation and tailing in the wild type or a *hen1* mutant. Dashed line on "Me" represents that miR158 is not fully methylated in the wild type; solid lines on "Me" on other miRNAs indicate that the methylation is lost in a *hen1* mutant. Different colors indicate different example miRNA families. nt, nucleotides.

DNA guide strand and target RNA reveal that base-pairing between guide strand and target occurs from positions 2 to 16 of the guide DNA strand (Wang et al., 2009), which may explain why many miRNAs in *hen1* are truncated to ~16 nucleotides before being tailed. Meanwhile, although animal miRNAs generally match poorly to their targets, it was proposed that differential miRNA-target pairing could affect a variety of allosteric changes on the Argonaute protein or RISC complex (Elkayam et al., 2012). Perhaps the RISC complex is programmed by the 3′ end of the loaded miRNA to direct specific patterns of 3′ modifications; consistent with this, a recent report illustrated that an asymmetric bulge on the miRNA/miRNA* duplex can program RISC during the loading step to enable the function of triggering secondary siRNA biogenesis (Manavella et al., 2012). Alternatively, the miRNA or miRNA–mRNA interactions may refine AGO1 physical or steric restrictions that impact 3′ modifications, as HESO1 can uridylate both the AGO1-bound miRNA as well as the cleaved target mRNA (G. Ren, M. Xie, C. Vinovskis, and B. Yu, unpublished data). We propose a model for AGO1 programming based on the differential patterns of miRNA modification that we observed in *Arabidopsis hen1* mutants (Figure 7). Such programming may not only impact the truncation and tailing (miR162, miR163, miR166, and miR171), but might also impact HEN1 activity on the terminal methylation of miRNA (e.g., miR158).

Patterns of truncation and tailing in a *hen1* background varied dramatically across miRNAs, ranging from those that are extremely truncated and tailed, such as miR166 and miR163, to those that are lacking evidence of substantial modification, like miR162; many miRNAs were in between these extremes. These patterns vary among miRNAs, yet are often similar for the same miRNA between monocots and dicots, which diverged ~200 million years ago (Nelson et al., 2004). The cross-species conservation of 3′ modifications of miRNAs suggests that it is the sequence of the mature miRNA that is the primary determinant of these modifications, both in the wild type and the *hen1* mutants. Loss-of-function mutations in the genes that catalyze truncation (possibly via *SDN1* and *2*) and uridylation (*HESO1*) have a clear impact on miRNA stability and accumulation (Ramachandran and Chen, 2008; Ren et al., 2012; Zhao et al., 2012b). Therefore, knowing that miRNAs vary substantially in numerous aspects of their biogenesis (e.g., expression, structure, processing, etc.), our data suggest that miRNAs also have different and specific fates for decay. We note that miR166 has a highly conserved 3′ end sequence ("CCCC"), which differs from most plant miRNAs and poorly matches its targets; perhaps in this case, the 3′ end is evolutionarily selected for, rather than better pairing to the target mRNAs, the definition of the miRNA decay destiny.

### Methylation as a Way to Modulate miRNA Accumulation

The modulation of miRNA accumulation through differential HEN1-dependent methylation is apparently rare in wild-type *Arabidopsis* (limited to miR158 and miR319 thus far). However, recent studies may suggest another biological role for this phenomenon. Pathogen-encoded transcription activator–like effectors can recognize specific DNA sequences with single nucleotide resolution through their repeat variable diresidues (Deng et al., 2012; Mak et al., 2012). Two different transcription activator–like effectors, Talc of *Xanthomonas oryzae* pv *oryzicola* and Tal9a of *X. oryzae* pv *oryzae*, are encoded by two distinct *Xanthomonas* strains yet share a common target: the promoter of the rice *HEN1* gene. These bacterial proteins target different regions of the same promoter, and both effectors dramatically enhance *HEN1* expression during infection (Moscou and Bogdanove, 2009). The reason for the induced overexpression of *HEN1* is as yet unknown, but perhaps this produces higher levels of HEN1 protein that may alter the relative abundance of miRNAs or other sRNAs significant to host responses. Perhaps *Xanthomonas* is thus exploiting *HEN1* and sRNA methylation to enhance the susceptibility of rice to the pathogen, as numerous sRNA-related cellular components are known to have a role in plant defenses (Katiyar-Agarwal and Jin, 2010). We believe that sRNA truncation and tailing, highly pronounced in the *hen1* mutants, is likely to have an important endogenous function in wild-type plants.

## METHODS

### Plant Materials

Immature inflorescence tissues, including inflorescence meristem, and early stage floral buds (up to stage 11/12) were collected from *Arabidopsis thaliana* grown in a growth chamber with 16 h of light for 5 weeks. For the seedling materials from the wild type, and the *ago1-11* and *hen1-2* single mutants, as well as the *ago1-11 hen1-2* double mutants, seeds were sterilized and plated on half-strength Murashige and Skoog medium containing 1% (w/v) Suc and 1% (w/v) agar. Plates were first kept in 4°C for 3 d and then moved to growth chamber and grown under continuous light. Whole-plant tissue samples were harvested 12 d after germination.

Rice plants containing the Os-*hen1* alleles *waf1-1* and *waf1-2* were grown in a growth chamber with 12 h of light for 5 weeks and genotyped by PCR to identify homozygous plants. The Os-*hen1-3* allele was identified from the Kyung Hee University T-DNA collection (Jeong et al., 2002) as line PFG_2C-00348; seeds were obtained and homozygous lines identified by PCR-based genotyping. For library construction, homozygous mutant seedlings at the 5-week stage were collected and the entire plants used for RNA extraction.

The Zm-*hen1-1* allele was isolated in W22 background with a Mu insertion (mu1007900) within the first exon of *HEN1*. This insertion was verified by PCR analysis and introgressed into B73. Materials were obtained from the homozygous F2 progeny derived from the W22 × B73 cross.

### RNA Extraction and Sequencing of sRNAs

Total RNA from the materials described above was isolated using Trizol reagents from Invitrogen. sRNA libraries were constructed using the Illumina TruSeq Small RNA Sample Preparation Kit (RS-200-0012) and sequenced on either an Illumina GAIIx or HiSeq2000 instrument at the Delaware Biotechnology Institute.

### RNA Gel Blotting, IP of AGO1, and Real-Time RT-PCR

RNA isolation and RNA gel blotting to detect sRNAs were performed as previously described (Park et al., 2002). Antisense DNA oligonucleotides that were 5′ end labeled (32P) were used to detect miRNAs. Sodium periodate treatment and β elimination were done as previously described

(Yu et al., 2005). The probe for detecting miR171a was 5′-GATATTGGCGCGGCTCAATCA-3′ (21 nucleotides); the probe for detecting miR158 was5′-GCTTTGTCTACATTTGGGA-3′ (19 nucleotides). IP was performed as previously described (Ji et al., 2011). The AGO1 mouse polyclonal antibody was generated in the Cao lab (Institute of Genetics and Developmental Biology, Chinese Academy of Sciences). Reverse transcription and real-time PCR were performed as previously described (Kim et al., 2011) with UBIQUITIN5 used as an internal control. Primers used to examine the expression of the miR158 target, AT3G03580, were described previously (Li et al., 2010).

### Bioinformatics Analysis of sRNAs

For sRNA reads that were not genome matched, one nucleotide was chopped off from the 3′ end in successive rounds until the remaining 5′ sequence was perfectly mapped to the *Arabidopsis* genome as previously described (Zhai and Meyers, 2013). Thus, any non-genome-matched sRNA read could be split into two parts: a 5′ head and a 3′ tail. The head portion of each read was aligned to all annotated *Arabidopsis* miRNAs in miRBase version 17 (Griffiths-Jones et al., 2008) for their origin, thus determining the extent of tailing (addition of nonconventional 3′ nucleotides) and truncation (shortening of the miRNA from the 3′ end). The head portion of reads was also mapped to the annotated transposable elements in TAIR (version 10; used only for its repeat data) to filter the transposable element–associated sRNAs used in Supplemental Figure 7 online, which were mostly ~24 nucleotides in the wild-type libraries. Genome-wide phasing analysis of sRNAs was performed as described previously (Zhai et al., 2011).

### Accession Numbers

The GenBank Gene Expression Omnibus accession number for the sRNA data described in Supplemental Table 1 online is GSE35562 (also found at http://smallrna.udel.edu/). Data for Columbia, *heso1-1*, *hen1-8*, and *heso1-1 hen1-8* libraries are from Zhao et al. (2012b). IP data from the wild type and catalytic mutants of AGO1 are from Carbonell et al. (2012).

### Supplemental Data

The following materials are available in the online version of this article.

**Supplemental Figure 1.** Characterization of New *hen1* Allele in Rice.

**Supplemental Figure 2.** Characterization of New *hen1* Allele in Maize.

**Supplemental Figure 3.** Size Distributions for Small RNA Sequencing Data.

**Supplemental Figure 4.** miRNAs are Differentially Truncated and Uridylated in *hen1* Mutants.

**Supplemental Figure 5.** miR171a Targets Produce 21 nt siRNAs in *hen1* Mutants.

**Supplemental Figure 6.** In *Arabidopsis*, AGO1 Binds to 3' Truncated and Tailed miRNAs.

**Supplemental Figure 7.** Size Distributions of Transposon-associated Small RNAs.

**Supplemental Table 1.** Summary of Small RNA Libraries from Plant *hen1* Mutants.

**Supplemental Table 2.** Truncated and Tailed Variants of miR166 in Diverse Plant Species.

**Supplemental Data Set 1.** Truncation and Tailing Patterns of Conserved miRNAs in *Arabidopsis hen1* Mutants.

**Supplemental Data Set 2.** Truncation and Tailing Patterns of Conserved miRNAs in Rice *hen1* Mutants.

### ACKNOWLEDGMENTS

This work was supported by the National Institute of Food and Agriculture, U.S. Department of Agriculture, under Agreement 2012-67013-19396, with additional support from the U.S. National Science Foundation Award 0701745. J.Z. was supported by a Graduate Fellow scholarship provided by the University of Delaware. Research in the Chen lab is supported by National Science Foundation Award 1021465 and by the Howard Hughes Medical Institute and Gordon and Betty Moore Foundation. Development of the AGO1 antibody in the Cao lab was supported by the National Natural Science Foundation of China (Award 30828002 to X.C.). Work in the Yang lab is supported by National Science Foundation Award 0820831, in the Yu lab by National Science Foundation Award 1121193, and in the Timmermans lab by National Science Foundation Award 1159098. We thank Tzuu-fen Lee from the Meyers lab and Yu Yu from the Chen lab for help in collecting plant materials. We also thank Jun-Ichi Itoh for providing the *waf1* mutant seeds and Gynheung An for providing the rice seeds later characterized as the Os-*hen1-3* line.

### AUTHOR CONTRIBUTIONS

J.Z. and B.C.M. designed research, performed research, contributed new computational methods, analyzed data. M.P. contributed new computational methods. S.A.S., S.H., K.P., S.A., L.J., M.X., Xf.C., B.Y., M.T., B.Y., and Xm.C. designed and performed research. All authors contributed to writing the article.

Received June 6, 2013; revised June 6, 2013; accepted June 20, 2013; published July 9, 2013.

### REFERENCES

**Abe, M., Yoshikawa, T., Nosaka, M., Sakakibara, H., Sato, Y., Nagato, Y., and Itoh, J.** (2010). WAVY LEAF1, an ortholog of *Arabidopsis* HEN1, regulates shoot development by maintaining microRNA and trans-acting small interfering RNA accumulation in rice. Plant Physiol. **154:** 1335–1346.

**Alefelder, S., Patel, B.K., and Eckstein, F.** (1998). Incorporation of terminal phosphorothioates into oligonucleotides. Nucleic Acids Res. **26:** 4983–4988.

**Ameres, S.L., Horwich, M.D., Hung, J.H., Xu, J., Ghildiyal, M., Weng, Z., and Zamore, P.D.** (2010). Target RNA-directed trimming and tailing of small silencing RNAs. Science **328:** 1534–1539.

**Bartel, D.P.** (2009). MicroRNAs: Target recognition and regulatory functions. Cell **136:** 215–233.

**Carbonell, A., Fahlgren, N., Garcia-Ruiz, H., Gilbert, K.B., Montgomery, T.A., Nguyen, T., Cuperus, J.T., and Carrington, J.C.** (2012). Functional analysis of three *Arabidopsis* ARGONAUTES using slicer-defective mutants. Plant Cell **24:** 3613–3629.

**Chen, H.M., Chen, L.T., Patel, K., Li, Y.H., Baulcombe, D.C., and Wu, S.H.** (2010). 22-Nucleotide RNAs trigger secondary siRNA biogenesis in plants. Proc. Natl. Acad. Sci. USA **107:** 15269–15274.

**Chen, X.** (2009). Small RNAs and their roles in plant development. Annu. Rev. Cell Dev. Biol. **25:** 21–44.

**Chen, X., Liu, J., Cheng, Y., and Jia, D.** (2002). HEN1 functions pleiotropically in *Arabidopsis* development and acts in C function in the flower. Development **129:** 1085–1094.

**Cuperus, J.T., Carbonell, A., Fahlgren, N., Garcia-Ruiz, H., Burke, R.T., Takeda, A., Sullivan, C.M., Gilbert, S.D., Montgomery, T.A.,**

**and Carrington, J.C.** (2010). Unique functionality of 22-nt miRNAs in triggering RDR6-dependent siRNA biogenesis from target transcripts in *Arabidopsis*. Nat. Struct. Mol. Biol. **17:** 997–1003.

**Deng, D., Yan, C., Pan, X., Mahfouz, M., Wang, J., Zhu, J.K., Shi, Y., and Yan, N.** (2012). Structural basis for sequence-specific recognition of DNA by TAL effectors. Science **335:** 720–723.

**Elkayam, E., Kuhn, C.D., Tocilj, A., Haase, A.D., Greene, E.M., Hannon, G.J., and Joshua-Tor, L.** (2012). The structure of human argonaute-2 in complex with miR-20a. Cell **150:** 100–110.

**Griffiths-Jones, S., Saini, H.K., van Dongen, S., and Enright, A.J.** (2008). miRBase: Tools for microRNA genomics. Nucleic Acids Res. **36** (Database issue)**:** D154–D158.

**Huang, Y., Ji, L., Huang, Q., Vassylyev, D.G., Chen, X., and Ma, J.B.** (2009). Structural insights into mechanisms of the small RNA methyltransferase HEN1. Nature **461:** 823–827.

**Hutvágner, G., McLachlan, J., Pasquinelli, A.E., Bálint, E., Tuschl, T., and Zamore, P.D.** (2001). A cellular function for the RNA-interference enzyme Dicer in the maturation of the let-7 small temporal RNA. Science **293:** 834–838.

**Jeong, D.H., An, S., Kang, H.G., Moon, S., Han, J.J., Park, S., Lee, H.S., An, K., and An, G.** (2002). T-DNA insertional mutagenesis for activation tagging in rice. Plant Physiol. **130:** 1636–1644.

**Ji, L., and Chen, X.** (2012). Regulation of small RNA stability: Methylation and beyond. Cell Res. **22:** 624–636.

**Ji, L., et al.** (2011). ARGONAUTE10 and ARGONAUTE1 regulate the termination of floral stem cells through two microRNAs in *Arabidopsis*. PLoS Genet. **7:** e1001358.

**Katiyar-Agarwal, S., and Jin, H.** (2010). Role of small RNAs in host-microbe interactions. Annu. Rev. Phytopathol. **48:** 225–246.

**Kim, Y.J., Zheng, B., Yu, Y., Won, S.Y., Mo, B., and Chen, X.** (2011). The role of Mediator in small and long noncoding RNA production in *Arabidopsis thaliana*. EMBO J. **30:** 814–822.

**Kim, Y.K., Heo, I., and Kim, V.N.** (2010). Modifications of small RNAs and their associated proteins. Cell **143:** 703–709.

**Kurihara, Y., and Watanabe, Y.** (2004). *Arabidopsis* micro-RNA biogenesis through Dicer-like 1 protein functions. Proc. Natl. Acad. Sci. USA **101:** 12753–12758.

**Li, J., Yang, Z., Yu, B., Liu, J., and Chen, X.** (2005). Methylation protects miRNAs and siRNAs from a 3′-end uridylation activity in *Arabidopsis*. Curr. Biol. **15:** 1501–1507.

**Li, Y., Zhang, Q., Zhang, J., Wu, L., Qi, Y., and Zhou, J.M.** (2010). Identification of microRNAs involved in pathogen-associated molecular pattern-triggered plant innate immunity. Plant Physiol. **152:** 2222–2231.

**Mak, A.N., Bradley, P., Cernadas, R.A., Bogdanove, A.J., and Stoddard, B.L.** (2012). The crystal structure of TAL effector PthXo1 bound to its DNA target. Science **335:** 716–719.

**Mallory, A.C., Reinhart, B.J., Jones-Rhoades, M.W., Tang, G., Zamore, P.D., Barton, M.K., and Bartel, D.P.** (2004). MicroRNA control of PHABULOSA in leaf development: Importance of pairing to the microRNA 5′ region. EMBO J. **23:** 3356–3364.

**Manavella, P.A., Koenig, D., and Weigel, D.** (2012). Plant secondary siRNA production determined by microRNA-duplex structure. Proc. Natl. Acad. Sci. USA **109:** 2461–2466.

**Mi, S., et al.** (2008). Sorting of small RNAs into *Arabidopsis* argonaute complexes is directed by the 5′ terminal nucleotide. Cell **133:** 116–127.

**Moscou, M.J., and Bogdanove, A.J.** (2009). A simple cipher governs DNA recognition by TAL effectors. Science **326:** 1501.

**Nelson, D.R., Schuler, M.A., Paquette, S.M., Werck-Reichhart, D., and Bak, S.** (2004). Comparative genomics of rice and *Arabidopsis*. Analysis of 727 cytochrome P450 genes and pseudogenes from a monocot and a dicot. Plant Physiol. **135:** 756–772.

**Park, W., Li, J., Song, R., Messing, J., and Chen, X.** (2002). CARPEL FACTORY, a Dicer homolog, and HEN1, a novel protein, act in microRNA metabolism in *Arabidopsis thaliana*. Curr. Biol. **12:** 1484–1495.

**Poethig, R.S.** (2009). Small RNAs and developmental timing in plants. Curr. Opin. Genet. Dev. **19:** 374–378.

**Qi, Y., He, X., Wang, X.J., Kohany, O., Jurka, J., and Hannon, G.J.** (2006). Distinct catalytic and non-catalytic roles of ARGONAUTE4 in RNA-directed DNA methylation. Nature **443:** 1008–1012.

**Ramachandran, V., and Chen, X.** (2008). Degradation of microRNAs by a family of exoribonucleases in *Arabidopsis*. Science **321:** 1490–1492.

**Ren, G., Chen, X., and Yu, B.** (2012). Uridylation of miRNAs by hen1 suppressor1 in *Arabidopsis*. Curr. Biol. **22:** 695–700.

**Schulze, S., Schäfer, B.N., Parizotto, E.A., Voinnet, O., and Theres, K.** (2010). LOST MERISTEMS genes regulate cell differentiation of central zone descendants in *Arabidopsis* shoot meristems. Plant J. **64:** 668–678.

**Voinnet, O.** (2009). Origin, biogenesis, and activity of plant microRNAs. Cell **136:** 669–687.

**Wang, Y., Juranek, S., Li, H., Sheng, G., Wardle, G.S., Tuschl, T., and Patel, D.J.** (2009). Nucleation, propagation and cleavage of target RNAs in Ago silencing complexes. Nature **461:** 754–761.

**Williams, L., Grigg, S.P., Xie, M., Christensen, S., and Fletcher, J.C.** (2005). Regulation of *Arabidopsis* shoot apical meristem and lateral organ formation by microRNA miR166g and its AtHD-ZIP target genes. Development **132:** 3657–3668.

**Xie, Z., Kasschau, K.D., and Carrington, J.C.** (2003). Negative feedback regulation of Dicer-Like1 in *Arabidopsis* by microRNA-guided mRNA degradation. Curr. Biol. **13:** 784–789.

**Yu, B., Bi, L., Zhai, J., Agarwal, M., Li, S., Wu, Q., Ding, S.W., Meyers, B.C., Vaucheret, H., and Chen, X.** (2010). siRNAs compete with miRNAs for methylation by HEN1 in *Arabidopsis*. Nucleic Acids Res. **38:** 5844–5850.

**Yu, B., Yang, Z., Li, J., Minakhina, S., Yang, M., Padgett, R.W., Steward, R., and Chen, X.** (2005). Methylation as a crucial step in plant microRNA biogenesis. Science **307:** 932–935.

**Zhai, J., et al.** (2011). MicroRNAs as master regulators of the plant NB-LRR defense gene family via the production of phased, trans-acting siRNAs. Genes Dev. **25:** 2540–2553.

**Zhai, J., and Meyers, B.C.** (February 7, 2013). Deep sequencing from hen1 mutants to identify small RNA 3′ modifications. Cold Spring Harb. Symp. Quant. Biol. **77:** 213–219.

**Zhao, Y., Mo, B., and Chen, X.** (2012a). Mechanisms that impact microRNA stability in plants. RNA Biol. **9:** 1218–1223.

**Zhao, Y., Yu, Y., Zhai, J., Ramachandran, V., Dinh, T.T., Meyers, B.C., Mo, B., and Chen, X.** (2012b). The *Arabidopsis* nucleotidyl transferase HESO1 uridylates unmethylated small RNAs to trigger their degradation. Curr. Biol. **22:** 689–694.

**Zilberman, D., Cao, X., Johansen, L.K., Xie, Z., Carrington, J.C., and Jacobsen, S.E.** (2004). Role of *Arabidopsis* ARGONAUTE4 in RNA-directed DNA methylation triggered by inverted repeats. Curr. Biol. **14:** 1214–1220.